Appl. Phys. A (2016) 122:488
DOI 10.1007/s00339-016-0024-9

Applied Physics A
Materials Science & Processing

The effect of pH on the synthesis of stable Cu_2O/CuO nanoparticles by sol–gel method in a glycolic medium

N. Zayyoun[1] · L. Bahmad[3] · L. Laânab[1] · B. Jaber[2]

Received: 23 September 2015 / Accepted: 24 March 2016 / Published online: 5 April 2016

Abstract In this work, we demonstrate that using a glycolic medium, both stable CuO and Cu_2O nanoparticles can be elaborated from Cu colloidal particles by adjusting their chemical environment, in particular the acido-basicity of the solution. In this context, the effect of pH on the sol–gel synthesis of Cu_2O/CuO NPs was investigated. XRD results confirmed the formation of pure Cu_2O with a cubic structure at lower pH (pH $\leq$ 6), whereas the pure monoclinic CuO was formed at higher pH (pH $\geq$ 12). TEM image indicates that the as-formed CuO NPs in basic pH are spherical in shape and their average size is found to be in the range of 4.5 nm. However, the as-obtained Cu_2O NPs in acid pH are cubical, with an average diameter of about 3 nm, and agglomerated into large spherical particles under the effect of ethylene glycol. Using the UV–Vis spectroscopy, the measured band gap energies of the prepared Cu_2O and CuO NPs are 2.07 and 4.08 eV respectively. FTIR results confirm the purity of the synthesized CuO and Cu_2O nanoparticles.

✉ N. Zayyoun
najouazayyoun@gmail.com

[1] LCS, Faculty of Sciences, Mohammed V University, Rabat, Morocco

[2] Material Science Platform, UATRS Division, CNRST, Rabat, Morocco

[3] LMPHE, Faculty of Sciences, Mohammed V University, Rabat, Morocco

1 Introduction

In recent years, metal oxides nanoparticles have attracted considerable attention on account of their potential applications and unique physical and chemical properties, which are strongly influenced by their size, morphology, and structure [1–3]. The synthesis of high-quality oxides with a controlled size and shape has been a major research focus in nanomaterials such as TiO_2 [4], ZnO [5], WO_3 [6], and SnO_2 [7].

Cupric oxide and cuprous oxide nanoparticles have attracted extensive attention in recent years because of their unique properties. CuO and Cu_2O are a p-type semiconductors with large band gaps (Eg (CuO) = 1.2 eV and Eg (Cu_2O) = 2 eV). Both materials present various applications, and CuO has been widely used in gas sensors [8], giant magneto-resistance materials [9, 10], field emission [11], nanofluid [12], lithium ion electrode materials [13], and nanodevices for catalysis [14], whereas Cu_2O has potential applications in solar energy [9], in gas sensing [15], photocatalysis [16–18], CO oxidation [19], photochemical evolution of hydrogen from water [20], and photocurrent generation [21, 22].

Many different chemical and physical methods have been reported to synthesize CuO; Wang et al. [23] prepared CuO nanorods by thermal decomposition. A new sonochemical method has been developed by Kumar et al. [24] to synthesize the copper oxide nanoparticles in various organic solvents such as DMF. Gedanken et al. [25] fabricated nanocrystalline CuO by a sonochemical method. While there are a little reported methods on the elaboration of pure Cu_2O nanostructures, it is difficult to synthesis this oxide in pure phase without any impurities due to the more stability of copper in Cu^{2+} state as compared to Cu^{1+}. Zheng et al. [26] prepared various shapes of Cu_2O

nanoparticles such as nanocube, cuboctahedra and truncated nanocubes by using PVP as a shape-directing agent and ascorbic acid as a reducing agent. Moreover, Murphy et al. [27] elaborated Cu_2O nanocubes by reduction of Cu^{2+} with sodium ascorbate. Furthermore, Yang et al. [28] synthesized Cu_2O and converted them into CuO NPs by gas-phase oxidation. Otherwise, Song et al. [29] demonstrated that an increase in the pH of solution allows the transformation of Cu_2O to CuO. However, all these methods either require high temperatures, long reaction time, sophisticated instrumentation, inert atmosphere or reducing agents to obtain these oxides in pure phases. Therefore, in the present study, we proposed a rapid one-step synthesis of stable CuO and Cu_2O nanoparticles using sol–gel method from the same copper acetate (CuAct2) as precursor and ethylene glycol (EG) as solvent. Moreover, until now, this procedure has not been reported in the literature for the elaboration of Cu_2O and CuO nanoparticles in a glycolic medium and in pure phases without introducing the reducing agents in the process. In this framework, the present paper aims to study the effect of the pH on the structural, morphological, and optical properties of the synthesized Cu_2O/CuO NPs.

2 Experimental details

All chemical products are of analytical grade purity. Cu_2O and CuO nanoparticles were synthesized using the sol–gel route. The typical experimental procedure is described as follows: 1.98 g of (Cu $(CH_3COO)_2$, H_2O) was dissolved into 100 ml of ethylene glycol and stirred for 1 h. Then, different concentrations of NaOH were added to the above solution at 60 °C under constant stirring during 2 h, and after that, the solution is cooled to room temperature in air. The resulting precipitates were filtered and washed twice with distilled water and once with absolute ethanol to remove all kinds of impurities and then dried at 50 °C.

A schematic of the process describing the main steps employed during the synthesis is depicted in Fig. 1.

3 Characterization

The crystalline phases were determined by X-ray diffractometer (XRD, Panalytical Xpert Pro) using CuKα as radiation source (45 kV, 40 mA). The nanoparticle size and morphology were carried out by transmission electron microscope (TEM, FEI Tecnai12 −120 kV). The UV–visible absorption spectrum of Cu_2O and CuO has been recorded by using UV–visible spectrophotometer (PerkinElmer Lambda 900), whereas the compositions of the products were analyzed by Fourier transform infrared (FTIR, Bruker Vertex) spectroscopy.

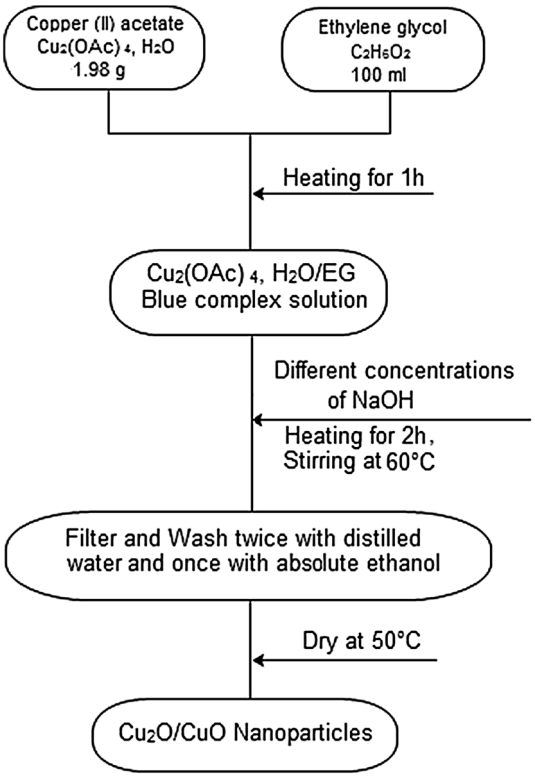

Fig. 1 Schema of the synthesis process of the CuO and Cu_2O NPs by sol–gel method

4 Results and discussion

4.1 Structural and morphological studies

A serie of experiments was carried out to synthesize Cu_2O and CuO nanoparticles from the same precursor and solvent by sol–gel method where the pH is the unique variable parameter. The temperature reaction was maintained at 60 °C. Table 1 presents the color of the synthesized powders as function of the final solution pH. The pH was increased from 6.1 to 12.5 by adding sodium hydroxide. At lower pH (pH < 7), an orange solution was formed which is a sign of the formation of the Cu_2O particles. However, when increasing the pH in the basic region, a blue color appeared indicating a change in the Cu^{2+} chemical environment. From pH = 12, the color of solution turns into black, which is a sign of the formation of the CuO particles.

X-ray diffraction characterizations of the obtained samples are given in Fig. 2. At acidic condition (pH = 6.1), the phase identification indicates that the as-

Table 1 Final pH of the solutions and crystalline structure associated with the color of the obtained powders

Sample number	pH	Powders color	Structure
1	6.1	Orange	Cu_2O
2	7.03	Deep green	($Cu_2C_2H_6O_5$, H_2O)
3	8.5	Bright blue	($CuC_4H_6O_4$, H_2O)/($CuC_4H_{12}O_2$)
4	12.5	Black	CuO

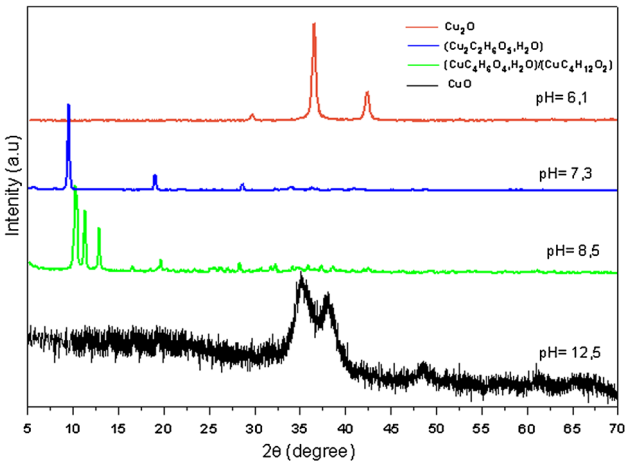

Fig. 2 X-ray diffraction patterns of the prepared samples at different pH values

formed sample is pure Cu_2O without any impurity peaks. All peaks are indexed to a cubic Cu_2O phase with the following cell constant: $a = 4.2626$ Å, which is consistent with the value of the JCPDS (card no. 01-077-0199). The peaks with 2θ values of 29.64°, 36.51°, 42.40°, and 52.63° correspond, respectively, to the atomic planes (111), (111), (200) and (211) of crystalline structure of Cu_2O. The recorded peak intensities clearly imply that the obtained powders are highly crystalline. By increasing the pH values, the XRD patterns show the phase transition leading to the formation of the copper-based secondary phases which are identified as following: ($Cu_2C_2H_6O_5$, H_2O) for the neutral pH and ($CuC_4H_6O_4$, H_2O)/($CuC_4H_{12}O_2$) for pH = 8.5. The XRD pattern shown in Fig. 2 indicates that the formation of the pure monoclinic CuO structure is only possible for the strongly basic solutions (pH ≥ 12). All diffraction peaks can be indexed as (110), (002), (111), (−202), (020), (202) and (−113) atomic plans using the JCPDS card no. 048–1548, and no other impurity peaks were detected. The calculated lattice parameters from XRD data are as follows: $a = 4.6863$ Å, $b = 3.4794$ Å and $c = 5.1226$ Å, which was in good agreement with literature.

Generally, the synthesis of cupric oxide and cuprous oxide nanoparticles by the sol–gel process is based on $Cu(OR)_2$ as a starting material [30]. It has been reported that CuO and Cu_2O particles grow through the dehydration–condensation reaction of $Cu(OH)_2$ species [31, 32]. In our case, where the precursor is the copper acetate monohydrate (Cu $(CH_3COO)_2$, H_2O), the followed mechanism is proposed to explain the formation of the obtained CuO and Cu_2O nanoparticles: The hydrolysis reaction:

$$OH - CH_2 - CH_2 - OH + Cu^{2+} \rightarrow [Cu(C_2H_6O)]^{2+} \quad (1)$$

The condensation process is initiated by NaOH addition:

$$[Cu(C_2H_6O)]^{2+} + 2OH^- \rightarrow Cu(OH)_2 + HOCH_2CH_2OH \quad (2)$$

At lower concentration of OH^-, the Cu_2O is firstly formed by dehydration of EG,

$$OHCH_2CH_2OH \rightarrow CH_3COH + H_2O \quad (3)$$

$$2Cu(OH)_2 + 2CH_3COH \rightarrow Cu_2O + CH_3 - CO - CO - CH_3 + 3H_2O \quad (4)$$

At higher concentration of OH^-, the $Cu(OH)_2$ is transformed into copper oxide phase,

$$Cu(OH)_2 \rightarrow CuO + H_2O \quad (5)$$

According to these equations, ethylene glycol (EG) and sodium hydroxide are the two key factors which orient the growth of CuO or Cu_2O nanostructures by controlling the pH medium. In the both cases (basic or acid), the stable complex $[Cu(II)EG]^{2+}$ is firstly formed after adding the ethylene glycol (EG) to the copper acetate according to Eq. (1) [33].

This complex is then transformed into $Cu(OH)_2$ by the addition of NaOH (Eq. 2).

When the pH value of the solution is too low (pH ≤ 6), the small concentration of OH^- in the solution is insufficient to form CuO nanoparticles. It is noted that the formation of CuO phases requires the presence of two OH^- for each Cu^{2+} in the solution as it has been reported in our previous work [34]. Consequently, the cubic Cu_2O (Eq. 4) is preferentially formed after the reduction of $Cu(OH)_2$ by the acetaldehyde molecules produced subsequently to the EG dehydration (Eq. 3) [33]. However, when the pH increases (pH ≥ 12), the high concentration of OH^- drives $Cu(OH)_2$ to dehydrate quickly and transforms into more stable CuO phase (Eq. 5). Figure 3 resumes the solution color variation which indicates the modification of copper-

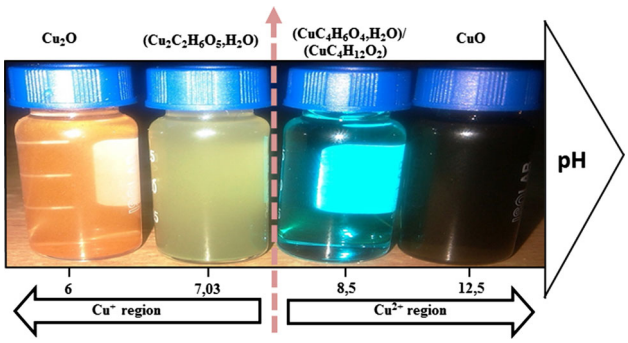

Fig. 3 Schema illustrating the color changes of the prepared glycolic solution when varying the pH

based chemical species present in the solution as a function of pH.

The morphological evolution and the size distribution of the as-prepared particles were examined by transmission electron microscope. The TEM image, illustrated in Fig. 4a, shows that the CuO nanoparticles are spherical in shape with uniform distribution and having an average diameter of 4.5 nm. These very small-sized particles tend to agglomerate under the effect of EG. The same result was also reported in the literature [35]. The morphology of the as-obtained Cu_2O powder, shown in TEM micrograph of Fig. 4b, consists of very small cubic particles with an average diameter of about 3 nm and aggregate into spherical shape under the effect of ethylene glycol. This formation in aggregation of Cu_2O nanoparticles is also observed in the literature [36].

4.2 Optical properties

To confirm the above result showed by XRD and TEM, CuO and Cu_2O nanoparticles were analyzed by FTIR spectroscopy. Figure 5a represents the FTIR spectrum of CuO NPs. The result shows three characteristic peaks of the vibrations of Cu–O observed at 420.7, 472, and 631.5 cm^{-1}, which is in good agreement with literature values. The high-frequency mode observed at 631.3 cm^{-1}

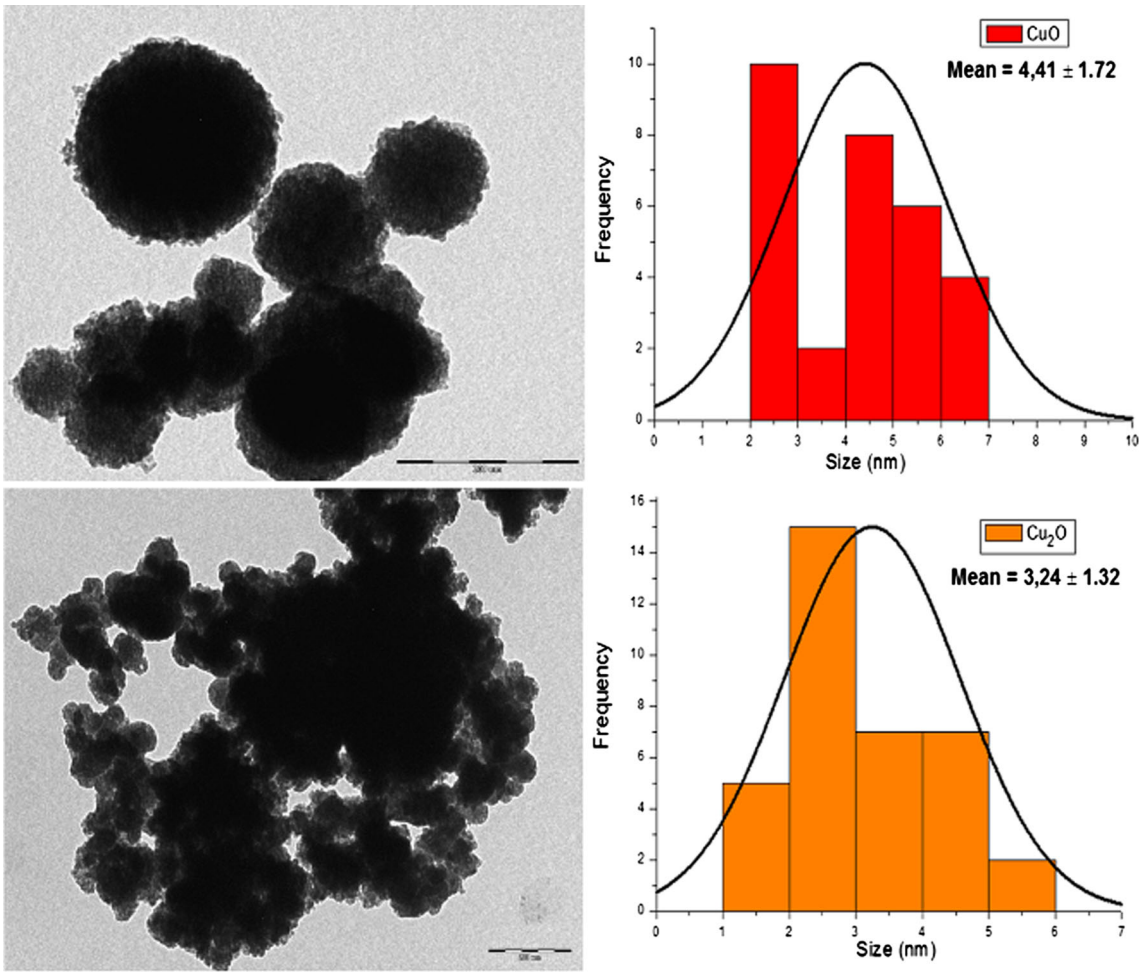

Fig. 4 TEM images and particle size distribution of **a** CuO NPs and **b** Cu_2O NPs

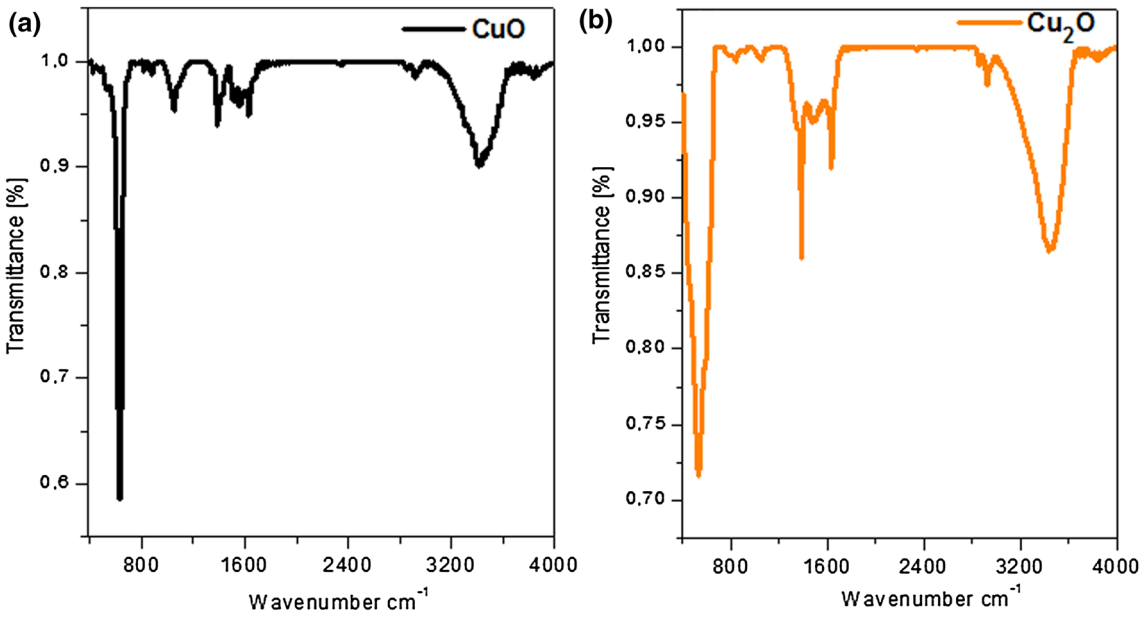

Fig. 5 FTIR spectra of copper oxides **a** CuO NPs and **b** Cu_2O NPs

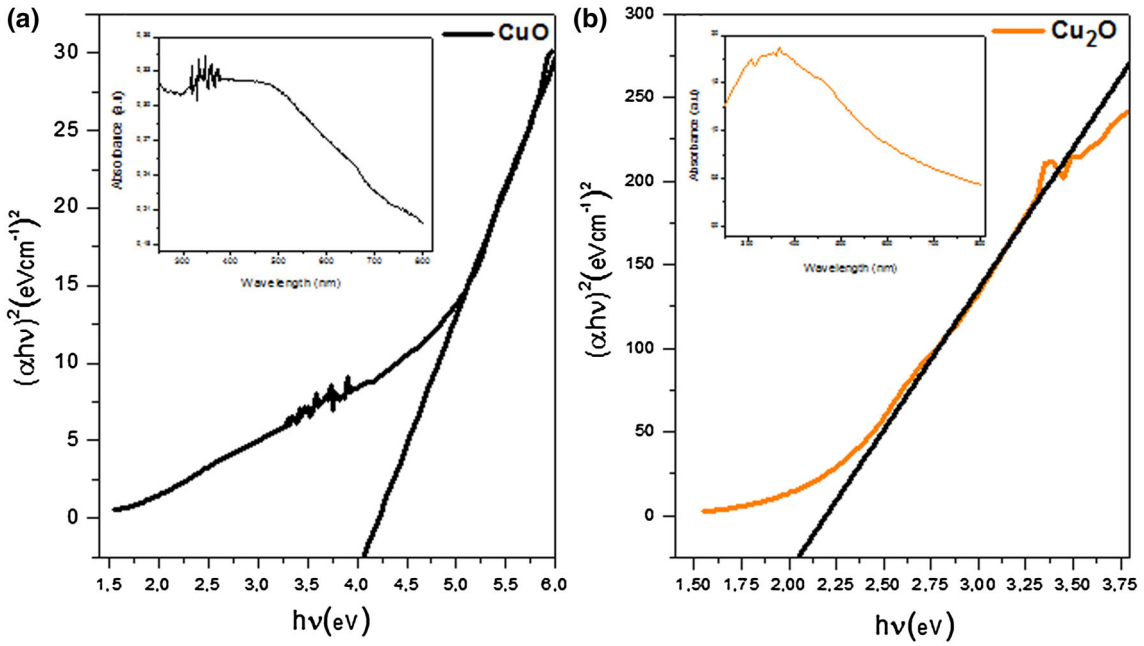

Fig. 6 UV–Vis spectra and Tauc's plots of CuO and Cu_2O NPs

in the spectrum is may be assigned to the vibration stretching along the Cu–O bond. However, the FTIR spectrum of Cu_2O nanoparticles (Fig. 5b) shows only one peak at about 533.6 cm^{-1} attributed to Cu–O vibration. The observation of the three peaks in the FTIR spectrum of CuO against one peak for Cu_2O confirms the formation of highly pure CuO and Cu_2O nanoparticles [37]. Compared with the bands of CuO/Cu_2O reported in the literature [38–40], the obtained peaks are downshifted due to nanosized effects.

Figure 6 displays the optical absorbance characteristics of Cu_2O and CuO nanostructures. As can be seen, an absorption peak is observed at 340 nm for Cu_2O and 350 nm for CuO. The direct band gap of these powders was determined from Tauc's plot [41]. The calculated band gap values are 4.08 eV and 2.07 eV for CuO and Cu_2O nanoparticles respectively (Fig. 6a and 6b). These values for both oxides are higher as compared to the bulk values (1.2 and 2 eV for CuO and Cu_2O, respectively). The

observed blueshift in the band gap is due to the quantum confinement effect [42]. The good obtained band gap values make Cu_2O and CuO nanoparticles relevant candidates for different solar energy harvesting and sensors applications.

5 Conclusion

In summary, a new process has been developed to prepare pure Cu_2O and CuO nanoparticles by sol–gel in the absence of surfactant agent or other additives. The results illustrated by XRD, TEM, and UV–Vis indicate that the pH of solution plays a vital role in the selection of the Cu_2O and/or CuO nanostructures phase formation. Pure CuO nanospheres and Cu_2O nanocubes are synthesized in the average sizes of 4.5 and 3 nm, respectively. The as-prepared CuO and Cu_2O possess very interesting optical properties (4.08 eV for CuO and 2.07 eV for Cu_2O), suggesting a promising interest in many applications such as the photoelectronic devices and harvesting solar energy.

References

1. M.A. El-Sayed, Acc. Chem. Res. **37**, 326 (2004)
2. A.P. Alivisatos, Endeavour **21**, 56 (1997)
3. A.P. Alivisatos, Science (1996). doi:10.1126/science.271.5251.933
4. X. Chen, S.S. Mao, Chem. Rev. **107**, 2959 (2007)
5. Z.L. Wang, J. Phy. Condens. Matter **16**, 858 (2004)
6. H. Zheng, J.Z. Ou, M.S. Strano, R.B. Kaner, A. Mitchell, K. Kalantar-zadeh, Adv. Funct. Mater. (2011). doi:10.1002/adfm.201002477
7. J. Pan, H. Shen, S. Mathur, J. Nanotechnol. (2012). doi:10.1155/2012/917320
8. A. Cruccolini, R. Narducci, R. Palombari, Sens. Actuators B: Chemical (2004). doi:10.1016/j.snb.2003.10.012
9. A.O. Musa, T. Akomolafe, M.J. Carter, Sol. Energy Mater. Sol. Cells **51**, 305 (1998)
10. X.G. Zheng, C.N. Xu, Y. Tomokiyo, E. Tanaka, H. Yamada, Y. Soejima, Phys. Rev. Lett. **85**, 5170 (2000)
11. X. Zhang, D. Zhang, X. Ni, H. Zheng, Solid-State Electronics **52**, 245 (2008)
12. L.P. Zhou, B.X. Wang, X.F. Peng, X.Z. Du, Y.P. Yang, Adv. Mech. Eng. (2010). doi:10.1155/2010/172085
13. S. Seung-Deok, J. Yun-Ho, L. Seung-Hun, S. Hyun-Woo, K. Dong-Wan, Nanoscale Res. Lett. **6**, 2 (2011)
14. Y. Jiang, S. Decker, C. Mohs, K.J. Klabunde, J. Catal. **180**, 24 (1998)
15. C.H.B. Ng, W.Y. Fan, J. Phys. Chem. B **110**, 20801 (2006)
16. C.-H. Kuo, M.H. Huang, J. Phys. Chem. C **112**, 18355 (2008)
17. J.-Y. Ho, M.H. Huang, J. Phys. Chem. C **113**, 14159 (2009)
18. C.-H. Kuo, C.-H. Chen, M.H. Huang, Adv. Funct. Mater. **17**, 3773 (2007)
19. B. White, M. Yin, A. Hall, D. Le, S. Stolbov, T. Rahman, N. Turro, S. O'Brien, Nano Lett. **6**, 2095 (2006)
20. M. Hara, T. Kondo, M. Komoda, S. Ikeda, J.N. Kondo, K. Domen, K. Shinohara, A. Tanaka, Chem. Commun. (1998). doi:10.1039/A707440I
21. C.M. McShane, K.S. Choi, J. Am. Chem. Soc. **131**, 2561 (2009)
22. Z. Yang, C.K. Chiang, H.T. Chang, Nanotechnology (2008). doi:10.1088/0957-4484/19/02/025604
23. C. Xu, Y. Liu, G. Xu, G. Wang, Mater. Res. Bull. **37**, 2365 (2002)
24. R.V. Kumar, Y. Diamant, A. Gendanken, Chem. Mater. **12**, 2301 (2000)
25. R.V. Kumar, Y. Diamant, A. Gendanken, R. Elgamiel, Langmuir **17**, 1406 (2001)
26. H. Xu, W. Wang, W. Zhu, Micro. Meso. Mater. **95**, 321 (2006)
27. L. Gou, C. Murphy, J. Nano Lett. **3**, 231 (2003)
28. J. Zhang, J. Liu, Q. Peng, X. Wang, Y. Li, Chem. Mater. **18**, 867 (2006)
29. J.C. Park, J. Kim, H. Kwon, H. Song, Adv. Mater. **21**, 803 (2009)
30. Brinker J, Scherer GW (1990) Academic Press, New York
31. W.Z. Wang, O.K. Varghese, C.M. Ruan, M. Paulose, C.A. Grimes, J. Mater. Res. **18**, 2756 (2003)
32. A. Li, P. Li, J. Hu, W. Zhang, J. Mater. Sci.: Mater. Electron. **26**, 5071 (2015)
33. X. Deng, Q. Zhang, Q. Zhao, L. Ma, M. Ding, X. Xu, Nanoscale Res. Lett. **10**, 2 (2015)
34. B. Jaber, L. Laânab, Mater. Sci. Semicond. Process. **27**, 446 (2014)
35. M. Cao, C. Hu, Y. Wang, Y. Guo, C. Guo, E. Wang, Chem. Commun. **15**, 1884 (2003)
36. S. Pande, S. Jana, A.K. Sinha, A. Datta, T. Pal, J. Phys. Chem. C **112**, 3619 (2008)
37. M. Kooti, L. Matouri, Tran. F : Nanotechnology **17**, 73 (2010)
38. G. Kliche, Z.V. Popovic, Phys Rev B **42**, 10060 (1990)
39. Y.C. Zhang, J.Y. Tang, G.L. Wang, M. Zhang, X.Y. Hu, J. Cryst. Growth **294**, 278 (2006)
40. I. Prakash, P. Muralidharan, N. Nallamuthu, M. Venkateswarlu, N. Satyanarayana, Mater. Res. Bull. **42**, 1619 (2007)
41. O. Game, U. Singh, A.A. Gupta, A. Suryawanshi, A. Banpurkar, S. Ogale, J. Mater. Chem. **22**, 17302 (2012)
42. A. Patra, K. Rajesh, T.P. Radhakrishnan, Bull. Mater. Sci. **31**, 421 (2008)